OXFORD JOURNALS
Bioinformatics

A single-array preprocessing method for estimating full-resolution raw copy numbers from all Affymetrix genotyping arrays including GenomeWideSNP 5 & 6

Journal:	*Bioinformatics*
Manuscript ID:	draft
Category:	Original Paper
Date Submitted by the Author:	n/a
Complete List of Authors:	Bengtsson, Henrik; University of California, Berkeley, Department of Statistics Wirapati, Pratyaksha; Swiss Institute of Experimental Cancer Research, National Center of Competence in Research Molecular Oncology; Swiss Institute of Bioinformatics, Bioinformatics Core Facility Speed, Terry; University of California, Berkeley, Department of Statistics; Walter & Eliza Hall Institute of Medical Research, Bioinformatics Division
Keywords:	copy number, microarray, Software, DNA, SNPs
Note: The following files were submitted by the author for peer review, but cannot be converted to PDF. You must view these files (e.g. movies) online.	
BengtssonH_2008c-CRMAv2.tex	

BIOINFORMATICS

Vol. 00 no. 00 2005
Pages 1–7

A single-array preprocessing method for estimating full-resolution raw copy numbers from all Affymetrix genotyping arrays including GenomeWideSNP 5 & 6

Henrik Bengtsson [a]*, Pratyaksha Wirapati [b,c], Terence P. Speed [a,d]

[a] Department of Statistics, University of California, Berkeley, USA. [b] National Center of Competence in Research Molecular Oncology, Swiss Institute of Experimental Cancer Research, Epalinges, Switzerland. [c] Bioinformatics Core Facility, Swiss Institute of Bioinformatics, Lausanne, Switzerland. [d] Bioinformatics Division, Walter & Eliza Hall Institute of Medical Research, Parkville, Australia.

Version: 2008-11-04 12:24; Received on XXXXX; revised on XXXXX; accepted on XXXXX

Associate Editor: XXXXXXX

ABSTRACT

Motivation: High-resolution copy-number (CN) analysis have in recent years gained much attention, not only for the purpose of identifying CN aberrations associated with a certain phenotype but also for identifying CN polymorphisms. In order for such studies to be successful and cost effective, the statistical methods have to be optimized. We propose a single-array preprocessing method for estimating full-resolution total CNs. It is applicable to all Affymetrix genotyping arrays, including the recent ones that also contain non-polymorphic probes. A reference signal is only needed at the last step when calculating relative CNs.

Results: As with our method for earlier generations of arrays, this one controls for allelic crosstalk, probe affinities and PCR fragment-length effects. Additionally, it also corrects for probe-sequence effects and co-hybridization of fragments digested by multiple enzymes that takes place on the latest chips. Using sex-chromosome HapMap data, we compare our method with Affymetrix' CN5 method and the dChip method, by assessing how well they differentiate between zero (CN=0), one (CN=1) and two (CN=2) copies at the full resolution and various amounts of smoothing. Although the others use data from all arrays for their preprocessing, CRMA v2 outperforms them for separating CN=1 from CN=2, and performs as well as CN5 for separating CN=0 from CN=1. This shows that it is possible to do online analysis in large-scale projects where additional arrays are introduced over time.

Availability: A bounded-memory implementation that can process any number of arrays is available in the open-source *R* package *aroma.affymetrix*.

Contact: hb@stat.berkeley.edu

1 INTRODUCTION

Following the suite of single-nucleotide polymorphism (SNP) arrays ('10K', '100K' and '500K'), Affymetrix has released a new class of chip types referred to as GenomeWideSNP ('GWS'), which in addition to SNP units include non-polymorphic probes, also called copy-number (CN) probes. The latter can be used to estimate the amount of target DNA at loci other than SNPs. The GenomeWideSNP_5 ('GWS5'), released February 2007, is targeted by Affymetrix as a genotyping assay, whereas the GenomeWideSNP_6 ('GWS6'), released May 2007, is targeted as both a genotyping and a CN assay.

In this paper we present the CRMA v2 method for estimating full-resolution raw total copy numbers (CNs). It extends and improves upon CRMA (Bengtsson *et al.*, 2008b) and applies to all Affymetrix genotyping arrays including GWS and custom arrays. Likewise, it does not require genotype calls. It should be emphasized that the purpose of the method is to provide better raw full-resolution estimates that increase chances for downstream methods such as segmentation methods and CN calling methods to produce better estimates.

In contrast to other methods, CRMA v2 is a single-array method that processes each array independently of the others. In order to achieve this, we had to overcome the challenges in adapting CRMA's multi-array steps. The access to a single-array preprocessing method has several implications: (i) Only two hybridizations are required for paired analysis, e.g. in a single-person tumor-normal study. (ii) Each array can be preprocessed immediately after being scanned. (iii) Arrays can be processed in parallel on different hosts/processors making it possible to decrease the processing time of a set of arrays linearly with the number of processors. (iv) There is no need to reprocess an array when new arrays are produced, which further saves time and computational resources. Furthermore, (v) the decision to filter out poor arrays can be made later, because a poor array will not affect the preprocessing of other arrays. More importantly, a single-array method is (vi) potentially very practical for applied medical diagnostics, because individual patients can be analyzed at once, even when they come singly rather than in batches.

The outline of this paper is as follows. In Methods, we start by describing important differences between the new GWS arrays and the former SNP arrays. In light of this, we explain how the original CRMA model is adapted for GWS, and how it is further

*To whom correspondence should be addressed

enhanced by introducing a normalization step controlling for probe-sequence effects. Each step is modified so that it can be applied to an array independently of the others. At the end of this section the evaluation method used for comparing with existing methods is described. In Results, we compare the different methods based on their performances at different levels of resolution and stratified by SNP or CN loci. In the Discussion, we conclude the study and give future research directions.

2 METHODS

2.1 Overview of the GWS arrays

The GWS6 chip type interrogates 931,946 SNPs and 945,826 CN loci totaling 1,877,772 loci, whereas GWS5 interrogates 500,568 SNPs and 417,269 CN loci totaling 917,837 unique loci. GWS5 has the same set of SNPs as the 500K chip set, whereas for GWS6 6,238 of those have been replaced by a new set of 437,616 SNPs. Among CN loci, only 61,846 are identical on GWS5 and GWS6. In contrast to previous generation of chip types (Bengtsson *et al.*, 2008b), there are no mismatch but only perfect-match (PM) probes. On GWS5, all SNPs have 4 replicated (PM_A, PM_B) pairs. On GWS6 there are either 3 or 4 such pairs. These probe pairs are identical replicates, whereas before they were slightly shifted relative to the SNP position. For both GWS arrays, the pairs in each SNP were selected such that they optimized the genotype performance. For the GWS5 there was no constraint that the PM_A and PM_B sequences had to be aligned on the genome, causing 192,399 (38.4%) SNPs to have misaligned PM_A and PM_B. There was also no constraint that PM_A and PM_B should be on the same strand, resulting in 46,176 (9.22%) SNPs with PM_A and PM_B on opposite strands. These constraint were reintroduced for GWS6. More details on the GWS arrays are available in the Supplementary Materials.

For the 100K as well as the 500K SNP-only assays, DNA is prepared in two parallel processes, each digesting the DNA using a unique enzyme, amplifying the fragments by PCR, and hybridizing the products to separate arrays. In the GWS assays, which like 500K, uses enzymes *Nsp*I and *Sty*I, the two mixes of PCR products are no longer hybridized to separate arrays but instead to the same array (Affymetrix Inc., 2007a,b). Consequently, some of the SNP target DNA of PCR products originating from different restriction digestions (enzymes) will hybridize to the same probe. The non-polymorphic (CN) probes were designed to target DNA either from both enzymes or *Nsp*I exclusively, but not from *Sty*I alone. For an explanation of this and a summary of how many SNP and CN loci are targeted by the two enzymes, see Suppl. Materials.

Finally, for GWS5 and GWS6, Affymetrix has identified 59,744 (6.51% of all loci) and 25,346 (1.35%) SNPs, respectively, that do not meet their quality criteria (private communication). In order to differentiate between the filtered and non-filtered sets of loci, Affymetrix provides one "default" chip definition file (CDF) and one "full" CDF. Further details on the two types of CDFs is given in the Suppl. Materials.

2.2 Data set

GWS6 CEL files for the 30 male and 30 female CEU founders of The International HapMap Project (The International HapMap Consortium, 2003; Altshuler *et al.*, 2005) was used. Offspring were excluded in order to avoid biological relationships. Because female NA12145 has a low true ChrX CN level (Ting *et al.*, 2006), it was excluded in the evaluation. More details on the data can be found in the Suppl. Materials.

2.3 Proposed model

The CRMA v2 method takes an approach similar to CRMA (Bengtsson *et al.*, 2008b) for estimating total (non-polymorphic) CNs. The model for allelic-crosstalk calibration is adapted to GWS, because of the added non-polymorphic probes. After this calibration, we utilize a nucleotide-position model (Carvalho *et al.*, 2007) to normalize for small difference across arrays but also for allelic imbalances in PM_A and PM_B. In contrast to our previous multi-array model, we here use a single-array model to summarize the probes. At the end, PCR fragment-length normalization is updated to model the multi-enzyme hybridization. CRMA v2 was designed to be: (i) backward compatible with previous generations of arrays, (ii) prepared for future generations of arrays, (iii) sequential, so that it is easy to replace or add other steps, and (iv) such that each array can be processed independently of the others. The latter allows for online single-array CN analysis, which becomes more important as larger data sets are being generated and updated over time, as well as it allows for analyzing very small data sets. It is only in the last step while calculating *relative* CNs that a reference is needed. Although not discussed further in this paper, we also look toward a unified method for estimating allele-specific CNs.

2.3.1 Calibration for offset and crosstalk between alleles For reasons explained in Bengtsson *et al.* (2008b), the (PM_A,PM_B) signals are affected by allelic crosstalk. It was shown that correcting for crosstalk as well as offset significantly improved the ability to differentiate between CN states. The offset & crosstalk model introduced in Bengtsson *et al.* (2008b) needs to be modified for GWS arrays in order to control for offset in the new non-polymorphic probes. For SNPs, let $\mathbf{x}_{ijk} = (x_{ijkA}, x_{ijkB})$ and $\mathbf{y}_{ijk} = (y_{ijkA}, y_{ijkB})$ denote the true and the observed signals for probe pair (j,k) in SNP j, probe $k = 1, \ldots, K_j$, and sample $i = 1, \ldots, I$. Without loss of generality, assume that probes in each pair are ordered lexicographically by the SNP nucleotides, resulting in six possible pairs. For a particular pair, we model the allelic crosstalk and shift observed in $\{\mathbf{y}_{ijk}\}$ by an array-specific affine transformation as

$$\mathbf{y}_{ijk} = \mathbf{a}_i + \mathbf{S}_i \mathbf{x}_{ijk} + \boldsymbol{\varepsilon}_{ijk}, \tag{1}$$

where $\mathbf{a}_i = (a_{iA}, a_{iB})^T$ denotes the offset,

$$\mathbf{S}_i = \begin{bmatrix} S_{iAA} & S_{iAB} \\ S_{iBA} & S_{iBB} \end{bmatrix} \tag{2}$$

is the crosstalk matrix, and $\boldsymbol{\varepsilon}_{ijk} = (\varepsilon_{ijkA}, \varepsilon_{ijkB})^T$ is noise. The affine parameters in this model are estimated based on the subset $\mathcal{J}^*$ of loci that are likely to be copy neutral regardless of sample, i.e. ChrX and ChrY data are excluded. If some of the remaining loci are not copy neutral, we rely on robustness of the estimator to get unbiased estimates. Estimates of the true signals are obtained by backtransforming as

$$\hat{\mathbf{x}}_{ijk} = \hat{\mathbf{S}}_i^{-1}(\mathbf{y}_{ijk} - \hat{\mathbf{a}}_i). \tag{3}$$

For further details, see Bengtsson *et al.* (2008b). For other non-SNP probes, including CN probes, we estimate and correct for the offset as the weighted average of offsets across all six nucleotide pairs with weights inversely proportional to the number of data points in each group. The reason for calculating the offset this way is the belief that there is a dominant offset that is shared by all probes, e.g. scanner offsets (Bengtsson *et al.*, 2004), which is further strengthened by our parallel studies on Affymetrix resequencing arrays. This also suggests that the offsets in Eqn (1) should be symmetric and same for all six pairs, but for practical reasons (Bengtsson *et al.*, 2008b) we choose not to do this. Another difference from CRMA (v1) is that after correcting for offset, all probe signals are rescaled to have the same arbitrary average ($= 2200$). In Bengtsson *et al.* (2008b) this was done for each nucleotide pair separately, but if done introduces systematic biases between SNPs and CN loci due to enzymatic mixture imbalances.

2.3.2 Normalization for probe-sequence effects It has been shown that the affinity of a probe can be attributed to its sequence composition (Binder *et al.*, 2004; Zhang *et al.*, 2007; Carvalho *et al.*, 2007). As in Carvalho *et al.* (2007), we model the probe-sequence affinity as a function of nucleotide and position in order to control for (i) small fluctuations in probe affinities across arrays, and (ii) differences in PM_A and PM_B affinities. Consider all probes $k' = 1, \ldots, K'$ on the array and let $\mathbf{b}_{k'} = (b_{k',1}, b_{k',2}, \ldots, b_{k',25})$ be the probe sequence for probe k' with nucleotide $b_{k',t} \in \{A, C, G, T\}$ at position $t = 1, \ldots, 25$. According to the probe-position model (Carvalho *et al.*, 2007), the crosstalk and offset calibrated signals $\hat{x}_{ik'}$ for probe k' of a given array $i = 1, \ldots, I$, can be described (on the intensity scale) by:

$$\hat{x}_{ik'} = \rho_{ik'} \cdot \mu_{ik'} + \xi_{ik'}, \tag{4}$$

where $\mu_{ik'}$ is the overall mean signal, $\rho_{ik'} > 0$ is the array and sequence-specific affinity, and $\xi_{ik'}$ is noise. The affinities are modeled on the logarithmic scale as:

$$\log_2 \rho_{ik'} = \log_2 \rho_i(\mathbf{b}_{k'}) = \sum_{b \in \{A,C,G,T\}} \sum_{t=1}^{25} \mathbb{I}(b_{k',t} = b) h_{i,b}(t), \tag{5}$$

where $\{h_{i,b}(\cdot)\}_b$ are nucleotide-specific smooth functions and $\mathbb{I}(\cdot)$ is the indicator function. The model is constrained such that $\sum_{b \in \{A,C,G,T\}} h_{i,b}(t) = 0$ at each position t. We choose to model $\{h_{i,b}(\cdot)\}_b$ with cubic splines with 5 degrees of freedom (we get very similar results for 7 and 9 d.f.). The model is fitted on the logarithmic scale with non-positive signals excluded, and as before, only to the subset of probes that are expected to be copy neutral. Given estimates $\{\hat{h}_{i,b}(\cdot)\}_b$, *all* probe signals can be normalized as:

$$\tilde{y}_{ik'} = \hat{x}_{ik'} / \hat{\rho}_i(\mathbf{b}_{k'}), \tag{6}$$

where $\{\tilde{y}_{ik'}\}$ denotes the offset & crosstalk calibrated and probe-sequence normalized signals. As in Carvalho *et al.* (2007), we observe small systematic effects across arrays $\{h_{i,b}(\cdot)\}_b$, which introduce extra variance. In addition, the difference in affinity between PM_B and PM_A is $h_{i,b_B}(t) - h_{i,b_A}(t)$ where t is the SNP probe position. If not controlled for, it will bias heterozygote signals (AB) relative to homozygote signals (AA or BB), when calculating the total signals. We note that the latter effect can be controlled for by introducing a heterozygote component in the crosstalk model, but as argued in Bengtsson *et al.* (2008b) such an approach is likely to be sensitive to model errors, e.g. when there are a lot of CN aberrations which may be the case for some tumors.

2.3.3 Probe-level summarization With technically replicated probes, assuming the effect from neighboring probes is negligible, probe affinities used in multi-array summarization models (Bengtsson *et al.*, 2008b) will vanish. For these reasons, we consider the following single-array summarization estimates for total CNs:

$$\begin{aligned} \tilde{y}_{ijk} &= \tilde{y}_{ijkA} + \tilde{y}_{ijkB}, \\ \hat{\theta}_{ij} &= \text{median}_k\{\tilde{y}_{ijk}\}, \end{aligned} \tag{7}$$

where the median is calculated across all probe-pair sums $k = 1, \ldots, K_j$ in SNP j. Finally, for non-polymorphic loci, which are all single-probe units (as defined by the CDFs used here), we let

$$\hat{\theta}_{ij} = \tilde{y}_{ij1} \tag{8}$$

be the corresponding estimates for unit/probe j in sample i. If in future chip types, or related custom genotyping arrays, there are replicated non-polymorphic probes, Eqn (8) should be replaced by summaries as in Eqn (7).

2.3.4 Normalization for fragment-length effects Because fragments from two enzymes are hybridized to the same array for GWS, some probes will match fragments originating from both restriction digestions. See Suppl. Materials for details on how many SNP and CN loci are exclusively on *Nsp*I, on *Sty*I, and on both. For signals originating from only one of the digestions, we could, for each enzyme separately, apply the fragment-length normalization method proposed in Bengtsson *et al.* (2008b). However, because a signal that originates from both digestions consists of one *Nsp*I and one *Sty*I component, which each has been amplified differently, another method has to be used for such units. For this reason, we modify the method in Bengtsson *et al.* (2008b) as described next.

First, assume that the number of fragments obtained from digesting with a particular enzyme is independent of locus j. This assumption was implicit in Bengtsson *et al.* (2008b). Continuing, let λ_j^r be the length of the fragment that was digested by restriction enzyme $r \in \{\text{Nsp}, \text{Sty}\}$ and contains locus j. For sample $i = 1, \ldots, I$, assume that the amount of PCR amplification of a fragment from digestion with enzyme $r \in \{\text{Nsp}, \text{Sty}\}$ is proportional to $2^{h_i^r(\lambda_j^r)}$, where $h_i^r(\cdot)$ is a sample-specific smooth function on the logarithmic scale. Next, labeled PCR products of the two digestions are mixed together. Let $\rho_i^r > 0$ be the total amount of product for enzyme r in sample i *relative to the* Nsp*I enzyme*, such that $\rho_i^{\text{Nsp}} = 1$ for all samples. Furthermore, assume that the amount of target hybridized to a specific probe is proportional to the number of labeled sequences. When targets from more than one digestion (enzyme) hybridize to the same probe, assume there is no preference for either enzyme. Next, let $\kappa_i > 0$ be the overall efficiency of hybridization, scanning, image analysis etc. for array i *relative to the first array*, such that $\kappa_1 = 1$. Finally, define $g_i^r(\cdot)$ such that $2^{g_i^r(\lambda_j^r)} = \kappa_i \rho_i^r 2^{h_i^r(\lambda_j^r)}$ describes, as a scale factor, the overall systematic effect for locus j in sample i due to fragmentation, PCR amplification, mixing, hybridization and so on. To conclude, for a

probe interrogating sequences from both digestions, we assume that the signal for sample i at locus j is proportional to:

$$2^{g_i^{\text{Nsp}}(\lambda_j^{\text{Nsp}})} + 2^{g_i^{\text{Sty}}(\lambda_j^{\text{Sty}})} = \kappa_i \left(2^{h_i^{\text{Nsp}}(\lambda_j^{\text{Nsp}})} + \rho_i^{\text{Sty}} 2^{h_i^{\text{Sty}}(\lambda_j^{\text{Sty}})}\right) \quad (9)$$

We say that *the confounded fragment-length effect is additive on the intensity scale*. With this model, each fragment-length effect $\{g_i^r(\cdot)\}_r$ can be estimated from signals exclusively from a single digestion.

In Bengtsson *et al.* (2008b) we normalized the data toward target fragment-length effects estimated as the average effects across arrays. In the effort to avoid multi-array estimators in CRMA v2, we here normalize data toward fixed target effects. The choice of target functions is not important because the effects will cancel out when CN ratios relative to a reference is calculated. Using the notation of Bengtsson *et al.* (2008b), we use constant target functions $g_T^r(\lambda) = \log_2(2200)$, where 2200 was chosen arbitrary.

Define $\mathcal{J}^{\text{Nsp}}, \mathcal{J}^{\text{Sty}}, \mathcal{J}^{\text{Nsp}\cap\text{Sty}} \subset \mathcal{J}$ to be the subsets of loci that are exclusive to *Nsp*I, *Sty*I, and to both enzymes, respectively. In order to simplify the notation, we will use the same notation for the true and the estimated functions. The normalization algorithm for array $i = 1, \ldots, I$ is then:

1. For each enzyme $r \in \{\text{Nsp}, \text{Sty}\}$, fit a smooth spline $g_i^r(\cdot)$ robustly to $\{(\lambda_j^r, \log_2 \theta_{ij})\}$ based on copy-neutral loci $j \in \mathcal{J}^r \cap \mathcal{J}^*$ that are exclusive to restriction enzyme r. This constitutes the *fragment-length effect for enzyme r in sample i*.
2. For each enzyme $r \in \{\text{Nsp}, \text{Sty}\}$, calculate the *PCR discrepancies for sample i* based on *all loci* $j \in \mathcal{J}^r$ that are exclusive to restriction enzyme r as
$$\log_2 \hat{\delta}_{ij} = g_i^r(\lambda_j^r) - g_T^r(\lambda_j^r) \quad (10)$$
3. For remaining loci $j \in \mathcal{J}^{\text{Nsp}\cap\text{Sty}}$, calculate the discrepancies as
$$\log_2 \hat{\delta}_{ij} = g_i^{\text{Nsp}\cap\text{Sty}}(\lambda_j^{\text{Nsp}}, \lambda_j^{\text{Sty}}) - g_T^{\text{Nsp}\cap\text{Sty}}(\lambda_j^{\text{Nsp}}, \lambda_j^{\text{Sty}}) \quad (11)$$
where
$$g_i^{\text{Nsp}\cap\text{Sty}}(\lambda^{\text{Nsp}}, \lambda^{\text{Sty}}) = \log_2 \left[2^{g_i^{\text{Nsp}}(\lambda^{\text{Nsp}})} + 2^{g_i^{\text{Sty}}(\lambda^{\text{Sty}})}\right], \quad (12)$$
and $g_T^{\text{Nsp}\cap\text{Sty}}(\lambda^{\text{Nsp}}, \lambda^{\text{Sty}})$ defined analogously.
4. Finally, normalize all loci (on the intensity scale) by
$$\tilde{\theta}_{ij} = \hat{\theta}_{ij} / \hat{\delta}_{ij}. \quad (13)$$

Loci for which annotation is missing (Suppl. Materials) are rescaled such that their median signal equals the median of the other loci. For chip types such as 10K, 100K and 500K, where there are no multi-enzyme loci ($\mathcal{J}^{\text{Nsp}\cap\text{Sty}} = \emptyset$), Step 3 no longer applies and the method becomes effectively identical to the one presented in Bengtsson *et al.* (2008b) (if the target effect is estimated from the average array). Moreover, since each $g_i^r(\cdot)$ includes the term ρ_i^r, the above method will also control for imperfect mixing of enzyme products, which otherwise carry through introducing systematic effects in loci that originate from both digestions. Analogously, the scale differences between arrays, $\{\kappa_i\}$, are also controlled for.

2.3.5 Calculation of raw copy numbers As in Bengtsson *et al.* (2008b), we calculate raw CNs as the chip effect relative to a reference. This is the only step in CRMA v2 requiring a reference. We calculate the relative CN for sample i and locus j as:

$$C_{ij} = 2 \cdot \frac{\tilde{\theta}_{ij}}{\tilde{\theta}_{Rj}}, \quad (14)$$

where $\tilde{\theta}_{Rj}$ is the reference signal, which commonly is the robust average across samples and possibly corrected for the case that some data points are from non-copy-neutral loci, cf. Bengtsson *et al.* (2008b). Note that for paired studies such as tumor-normal comparisons, the normal DNA will serve as the reference, which is why only two hybridizations are needed in such comparisons. In Eqn (14) we assume that the mean of $\tilde{\theta}_{Rj}$ corresponds to $CN = 2$, e.g. ChrY reference estimates should be rescaled accordingly. For CN estimates on the logarithmic scale, we calculate:

$$M_{ij} = \log_2 \frac{\tilde{\theta}_{ij}}{\tilde{\theta}_{Rj}}. \quad (15)$$

Note that the latter is not defined for zero copy-number levels (or for negative levels occurring due to noise).

2.3.6 Filtered and non-filtered set of loci Regardless of whether CN analysis will be conducted on a filtered or the full set of loci, we recommend that all preprocessing is done on the full set and filtering is applied only after obtaining raw CNs. The rationale for this is that we believe the main systematic effects are the same for the filtered and the full set and that one can estimate these effects more accurately using the latter. This also has the advantage that the preprocessing will be the same regardless of which set is used in the end.

2.4 Implementation

The above preprocessing method, referred to as *CRMA v2*, is available as part of *aroma.affymetrix* (Bengtsson *et al.*, 2008a) implemented in *R* (R Development Core Team, 2008). The method is designed and implemented to have bounded-memory usage, regardless of the number of arrays. Since it is a single-array method, the arrays can be processed in parallel on multiple hosts/processors.

2.5 Methods for evaluation

In order to assess the performance of CRMA v2, we compared it with Affymetrix CN5 method (Affymetrix Inc., 2008) and the method implemented in dChip (Li and Wong, 2001). For *dChip*, we found that summarizing SNP probes by averaging is significantly better than using the default multiplicative model. For this reason, we only present results for the former (here denoted by *dChip**). We used the same set of evaluation methods as in Bengtsson *et al.* (2008b) using relative (Eqn (14)) instead of log-ratio CNs (Eqn (15)). To assess how well the methods differentiate between one and two copies, and zero and one copy, we use ChrX and ChrY data, respectively. We exclude loci in pseudo-autosomal regions (Blaschke and Rappold, 2006) and inside and close to known CN polymorphic regions (Redon *et al.*, 2006). Moreover, since the CN5 implementation is limited to the default CDF, the results presented here are based on that set of loci. Since CN5

uses only females (males) for the reference signals $\{\tilde{\theta}_{Rj}\}$ on ChrX (ChrY), this comparison study will not use bias-corrected reference signals from all samples (Bengtsson *et al.*, 2008b). For more details on the above, see Suppl. Materials.

3 RESULTS

3.1 Differentiating CN=1 and CN=2 (ChrX)

The true-positive rate of calling a CN=1 locus correctly (among CN=2 loci) as a function of false-positive rate is depicted in Figure 1 for each of the three methods. The ROC curves show that CRMA v2 separates CN=1 from CN=2 better than CN5, which in turn is better than dChip*. This is true both at the full resolution ($H = 1$) and at various amounts of smoothing. We also note that CRMA v2 smoothed with 3 loci per window performs equally well or better than dChip* smoothed with 4 loci per window (see also Figure 2).

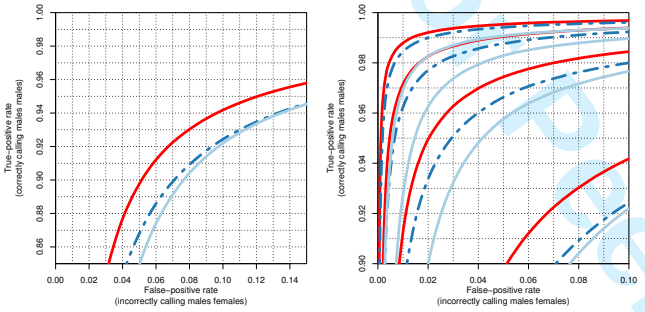

Fig. 1. ROC curves showing that CRMA v2 (solid red) separates CN=1 from CN=2 (ChrX) better than CN5 (dashed blue) and dChip* (solid light blue) at the full resolution ($H = 1$; left panel) as well as at various amounts of smoothing ($H = 1, 2, 3, 4$; right panel). The curves for $H = 1$ are in the lower right corner and the curves for $H = 4$ are in the upper left corner.

Using a windowing technique similar to that in Bengtsson *et al.* (2008b), for a fixed false-positive rate we can estimate the true-positive rate as a function of amount of smoothing. Since a given amount of smoothing corresponds to a given distance between loci this provides us with a first approximation to the effective resolution of a method. In the upper panel of Figure 2 the true-positive rate (for CN=2 v. CN=1) as a function of resolution is shown for the three methods, which shows that CRMA v2 has a higher resolution.

3.2 Differentiating CN=0 and CN=1 (ChrY)

Identifying a CN=0 locus among CN=1 loci is easier than identifying a CN=1 locus among CN=2 loci. This is because the distance between CN=0 and CN=1 is greater than that between CN=1 and CN=2, relative to the reference level (and noise level). This is also confirmed by comparing the corresponding true-positive rates at a given false-positive rate (Figure 1 and Figure 3) at the full resolution or at various amounts of smoothing (Figure 2). The results also show that CN5 is equally good or slightly better than CRMA v2 at differentiating CN=0 from CN=1, and both are better than dChip*.

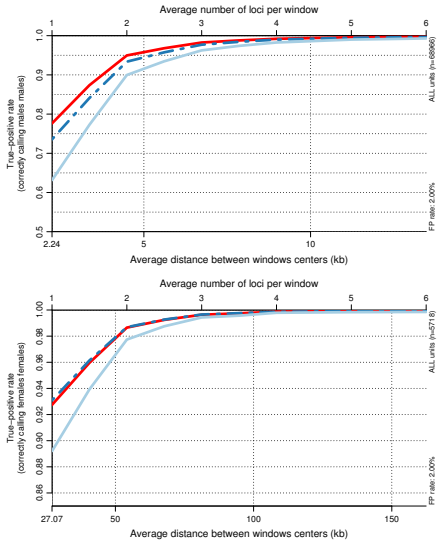

Fig. 2. The true-positive rate as a function of resolution/smoothing at a 2.0% false-positive rate for the different methods. The results for the CN=2 v. CN=1 (ChrX) test is depicted in the upper panel and the results for the CN=1 v. CN=0 (ChrY) test in the lower panel. Note the different scales. See Figure 1 for legends.

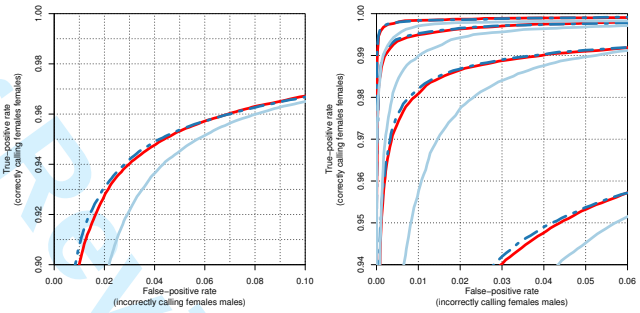

Fig. 3. ROC curves showing CRMA v2 differentiates between CN=1 and CN=0 (ChrY) equally well as or slight worse than CN5, and better than dChip* at the full resolution (left panel) as well as at various amounts of smoothing (right panel). See Figure 1 for legends.

3.3 Performance of SNPs and CN loci

In order to better understand differences between methods, we compare the ROC curves and distribution of true-positive rates at a given false-positive rate (Bengtsson *et al.*, 2008b) while stratifying on SNP and CN loci. We observe that on average the discriminatory power is greater for SNPs than CN loci (upper panels of Figure 4 and Figure 5). CN5 is the method for which SNPs and CN loci have the most similar performances. Furthermore, by investigating the locus-by-locus ROCs, we observe that the true-positive rates at a fixed false-positive rate tend to be greater for SNPs than for CN loci (lower panels), and that there is a significant set of CN loci with very low true-positive rates. The dChip* method has a larger set of poorly performing CN loci, which is also seen when comparing dChip's ROC curves for SNPs and CN loci.

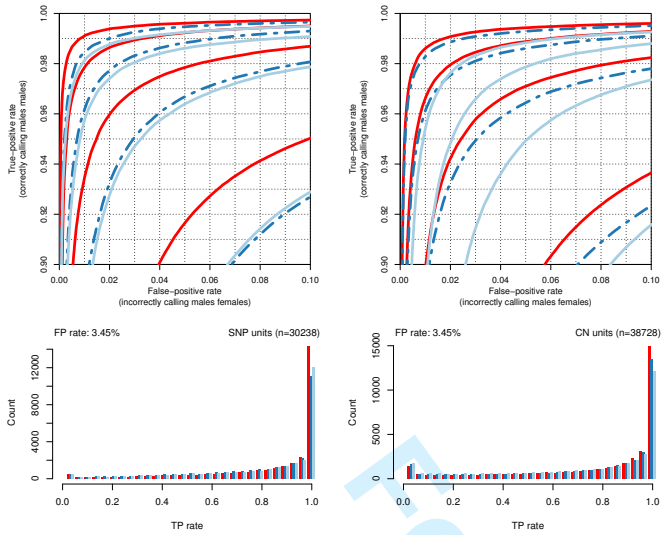

Fig. 4. Performance on SNPs (left) and CN units (right) for CRMA v2 (solid red; left bars), CN5 (dashed blue; middle bars) and dChip* (solid light blue; right bars) when testing for CN=2 v. CN=1 (ChrX). The upper panels show the ROC curves for $H = 1, 2, 3, 4$ and the lower panels show the distribution of true-positive rates at fixed false-positive rate (1.72%).

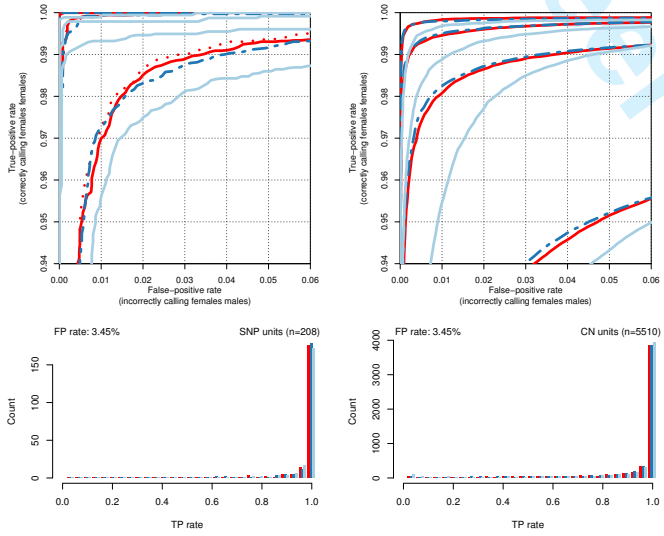

Fig. 5. Performance on SNPs (left) and CN units (right) for CRMA v2, CN5 and dChip* when testing for CN=1 v. CN=0 (ChrY). The upper panels show the ROC curves for $H = 1, 2, 3, 4$ and the lower panels show the distribution of true-positive rates at fixed false-positive rate (1.72%). Legends as in Figure 4.

4 DISCUSSION

We conclude that it is possible for a single-array method such as CRMA v2 to produce non-polymorphic CN estimates that discriminate two CN states equally well or better than existing multi-array based methods. Our study confirms that it is harder to differentiate between CN=1 and CN=2 than between CN=0 and CN=1. We believe that this trend will be true for higher CN levels, i.e. it will be harder and harder to separate higher CN levels from each other. We also found that the SNPs show stronger discrimination for copy number than the CN loci. We look forward to further studies investigating whether this is because more/multiple probes are used for the SNPs or there are other reasons for this. Also, it still has to be assessed how well CRMA v2 (and other methods) controls for systematic effects between labs and batches, and whether additional normalization is needed in such cases.

We also wish to emphasize that the dChip method has not been optimized for GWS or SNP arrays, which may explain its lower performance in this GWS6 study in comparison with its higher performance for the 500K arrays (Bengtsson *et al.*, 2008b).

CRMA v2 provides neither allele-specific nor calibrated CN estimates. Allele-specific CNs are needed in order to identify events such as copy-neutral loss-of-heterozygosity (LOH). With calibrated allele-specific CNs, genotyping algorithms can be generalized to call genotypes beyond the traditional diploid AA, AB, and BB states. We are currently working on an extension to CRMA v2 that will provide full-resolution calibrated allele-specific CN estimates.

ACKNOWLEDGEMENTS

We wish to thank Ben Bolstad, Simon Cawley, and Jim Veitch at Affymetrix Inc. for technical support and scientific feedback. We also thank Cheng Li at the Harvard School of Public Health for details on the dChip method and software. HB was supported by grants from the Wenner-Gren Foundation, the American-Scandinavian Foundation, and the Solander Foundation.

REFERENCES

Affymetrix Inc. (2007a). *Genome-Wide Human SNP Nsp/Sty 6.0 User Guide*. Affymetrix Inc. Rev 1.

Affymetrix Inc. (2007b). *Genome-Wide Human SNP Nsp/Sty Assay 5.0*. Affymetrix Inc. Rev 2.

Affymetrix Inc. (2008). *Affymetrix Genotyping Console 3.0 - User Manual*. Affymetrix Inc.

Altshuler, D., Brooks, L. D., Chakravarti, A., Collins, F. S., Daly, M. J., Donnelly, P., and Consortium, I. H. (2005). A haplotype map of the human genome. *Nature*, **437**(7063), 1299–1320.

Bengtsson, H., Jönsson, G., and Vallon-Christersson, J. (2004). Calibration and assessment of channel-specific biases in microarray data with extended dynamical range. *BMC Bioinfo.*, **5**, 177.

Bengtsson, H., Simpson, K., Bullard, J., and Hansen, K. (2008a). aroma.affymetrix: A generic framework in R for analyzing small to very large Affymetrix data sets in bounded memory. Technical Report 745, Department of Statistics, University of California, Berkeley.

Bengtsson, H., Irizarry, R. A., Carvalho, B., and Speed, T. P. (2008b). Estimation and assessment of raw copy numbers at the single locus level. *Bioinformatics*, **24**(6), 759–767.

Binder, H., Kirsten, T., Loeffler, M., and Stadler, P. F. (2004). Sensitivity of microarray oligonucleotide probes: Variability and

effect of base composition. *J.Phys.Chem B*, **108**(46), 18003–18014.

Blaschke, R. J. and Rappold, G. (2006). The pseudoautosomal regions, shox and disease. *Curr Opin Genet Dev*, **16**(3), 233–239.

Carvalho, B., Bengtsson, H., Speed, T. P., and Irizarry, R. A. (2007). Exploration, normalization, and genotype calls of high-density oligonucleotide SNP array data. *Biostatistics*, **8**(2), 485–499.

Li, C. and Wong, W. (2001). Model-based analysis of oligonucleotide arrays: expression index computation and outlier detection. *Proc. Natl. Acad. Sci. USA*, **98**(1), 31–6.

R Development Core Team (2008). *R: A Language and Environment for Statistical Computing*. R Foundation for Statistical Computing, Vienna, Austria. ISBN 3-900051-07-0.

Redon, R., Ishikawa, S., Fitch, K. R., Feuk, L., Perry, G. H., Andrews, T. D., and ... (2006). Global variation in copy number in the human genome. *Nature*, **444**, 444–454.

The International HapMap Consortium (2003). The International HapMap Project. *Nature*, **426**, 789–796.

Ting, J., Ye, Y., Thomas, G., Ruczinski, I., and Pevsner, J. (2006). Analysis and visualization of chromosomal abnormalities in SNP data with SNPscan. *BMC Bioinfo.*, **7**(1), 25.

Zhang, L., Wu, C., Carta, R., and Zhao, H. (2007). Free energy of dna duplex formation on short oligonucleotide microarrays. *Nucleic Acids Res*, **35**(3), e18.

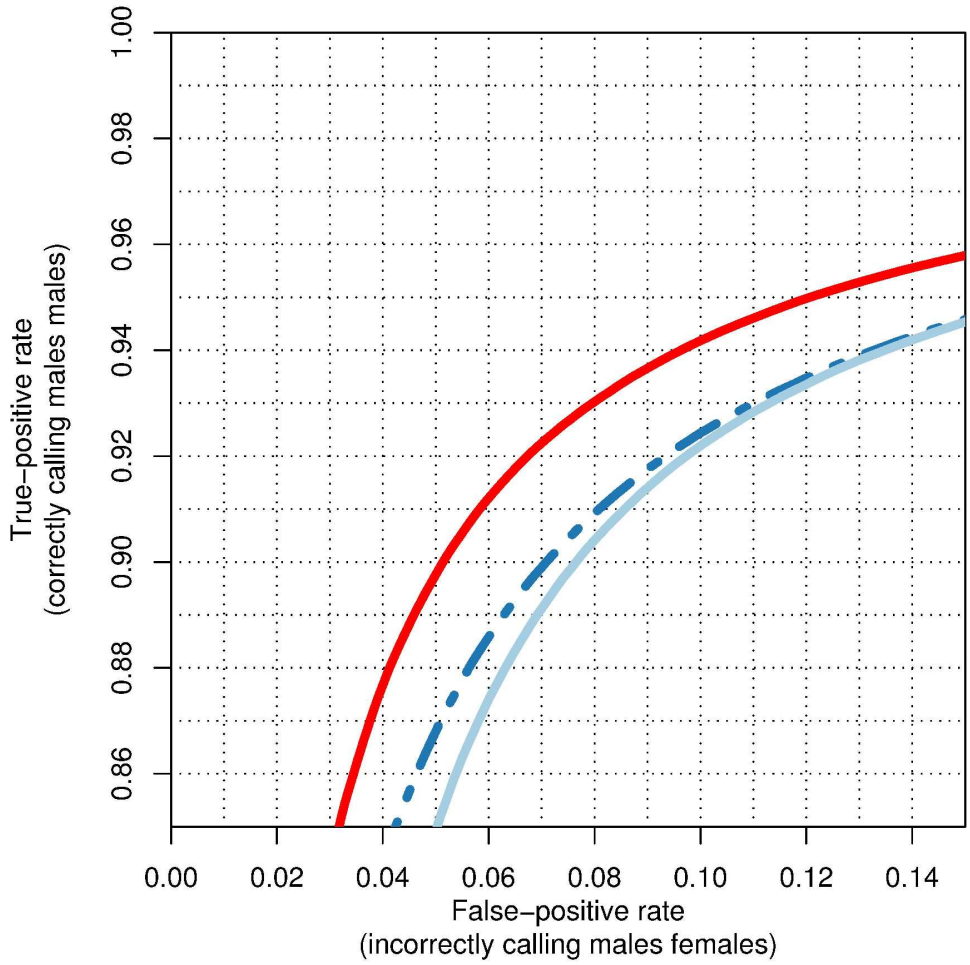

ROC curves showing that CRMA v2 (solid red) separates CN=1 from CN=2 (ChrX) better than CN5 (dashed blue) and dChip* (solid light blue) at the full resolution (H=1; left panel) as well as at various amounts of smoothing (H=1,2,3,4; right panel). The curves for H=1 are in the lower right corner and the curves for H=4 are in the upper left corner.
152x152mm (600 x 600 DPI)

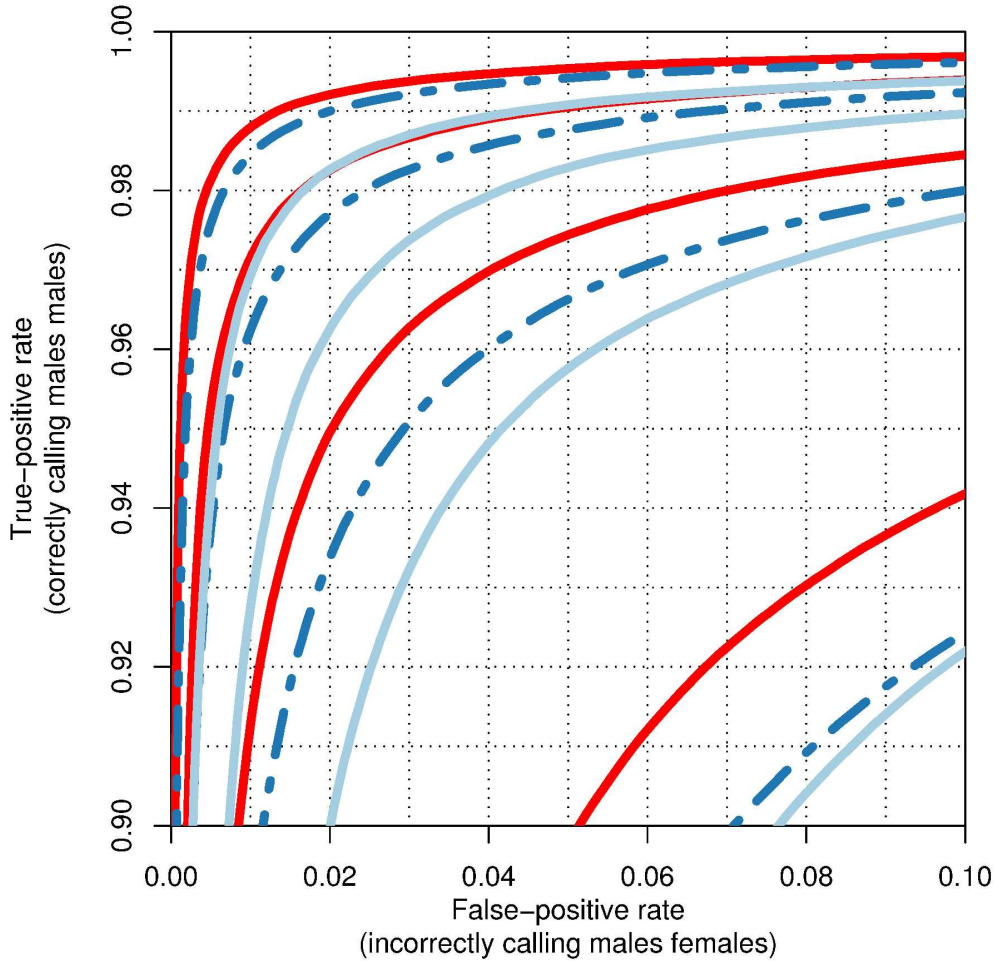

ROC curves showing that CRMA v2 (solid red) separates CN=1 from CN=2 (ChrX) better than CN5 (dashed blue) and dChip* (solid light blue) at the full resolution (H=1; left panel) as well as at various amounts of smoothing (H=1,2,3,4; right panel). The curves for H=1 are in the lower right corner and the curves for H=4 are in the upper left corner.
152x152mm (600 x 600 DPI)

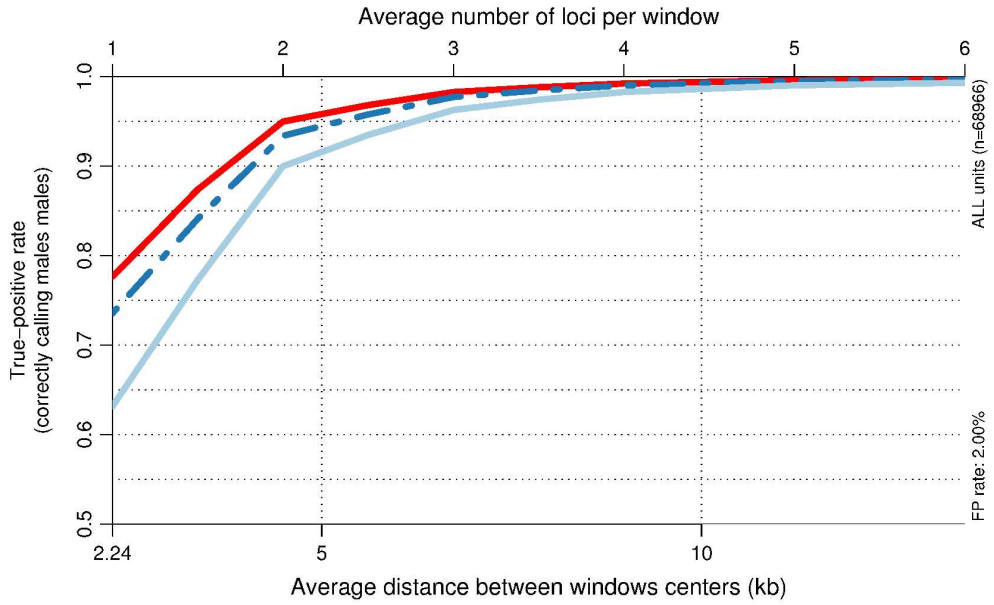

The true-positive rate as a function of resolution/smoothing at a 2.0% false-positive rate for the different methods. The results for the CN=2 v. CN=1 (ChrX) test is depicted in the upper panel and the results for the CN=1 v. CN=0 (ChrY) test in the lower panel. Note the different scales. See Figure 1 for legends.
213x131mm (600 x 600 DPI)

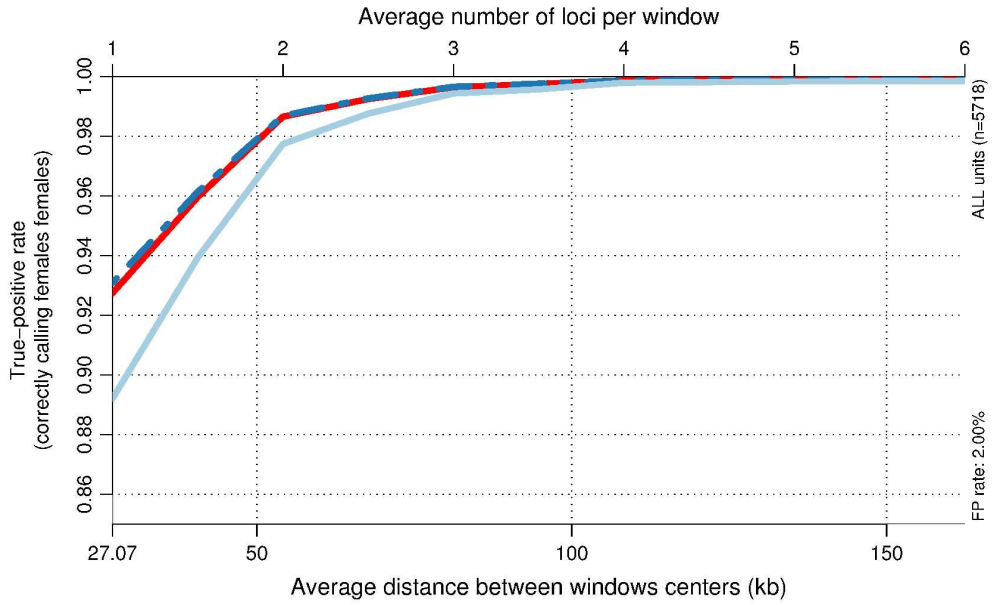

The true-positive rate as a function of resolution/smoothing at a 2.0% false-positive rate for the different methods. The results for the CN=2 v. CN=1 (ChrX) test is depicted in the upper panel and the results for the CN=1 v. CN=0 (ChrY) test in the lower panel. Note the different scales. See Figure 1 for legends.
213x131mm (600 x 600 DPI)

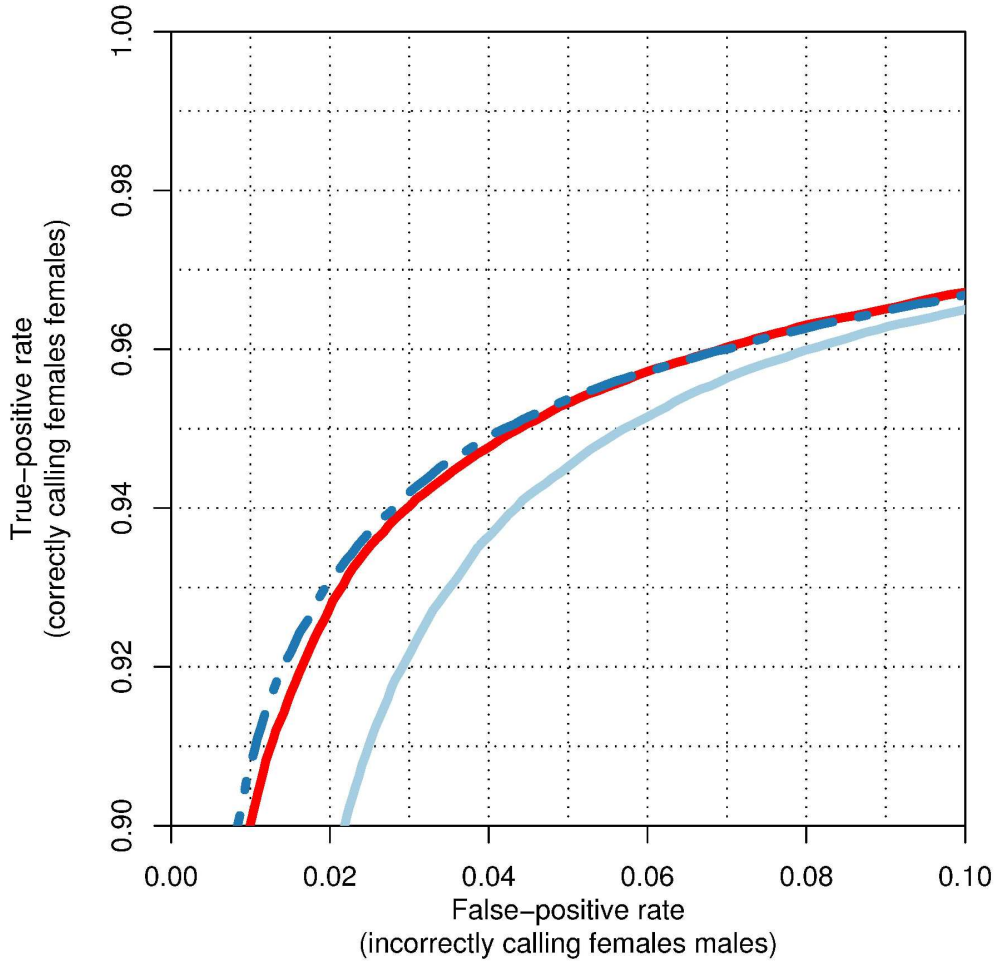

ROC curves showing CRMA v2 differentiates between CN=1 and CN=0 (ChrY) equally well as or slight worse than CN5, and better than dChip* at the full resolution (left panel) as well as at various amounts of smoothing (right panel). See Figure 1 for legends.
152x152mm (600 x 600 DPI)

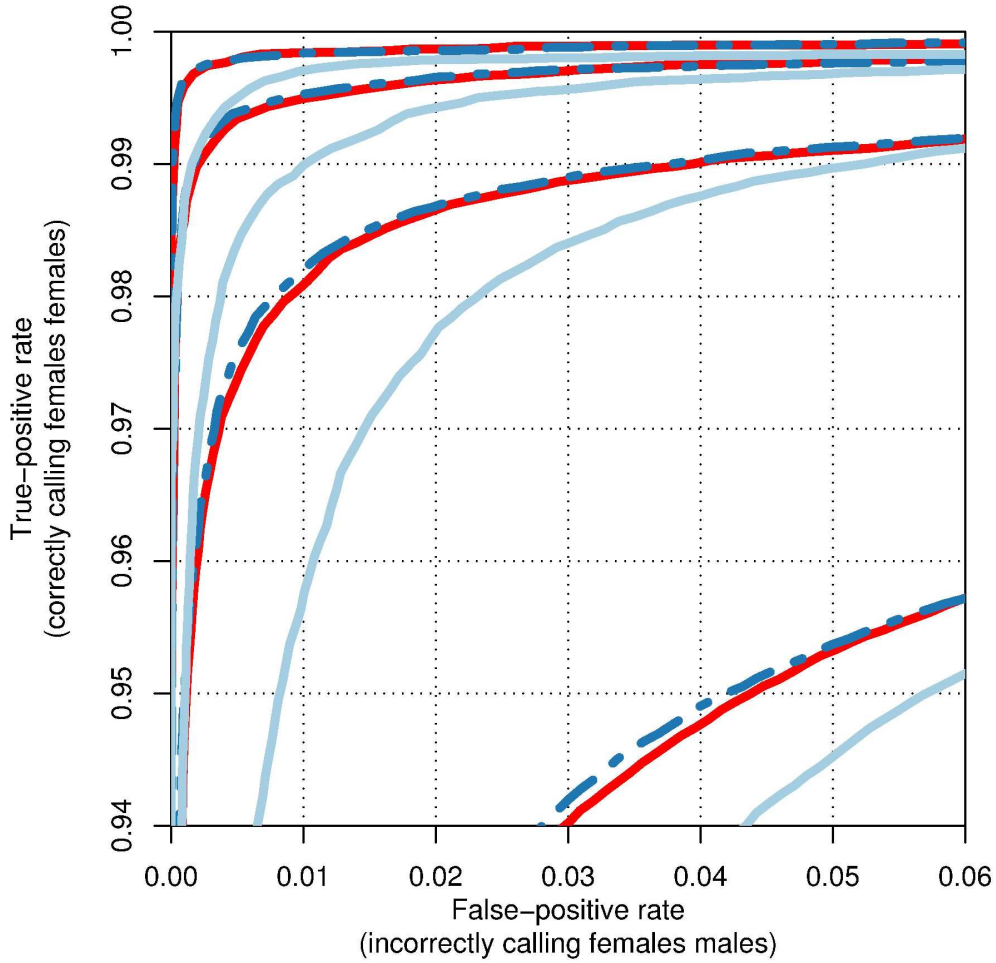

ROC curves showing CRMA v2 differentiates between CN=1 and CN=0 (ChrY) equally well as or slight worse than CN5, and better than dChip* at the full resolution (left panel) as well as at various amounts of smoothing (right panel). See Figure 1 for legends.
152x152mm (600 x 600 DPI)

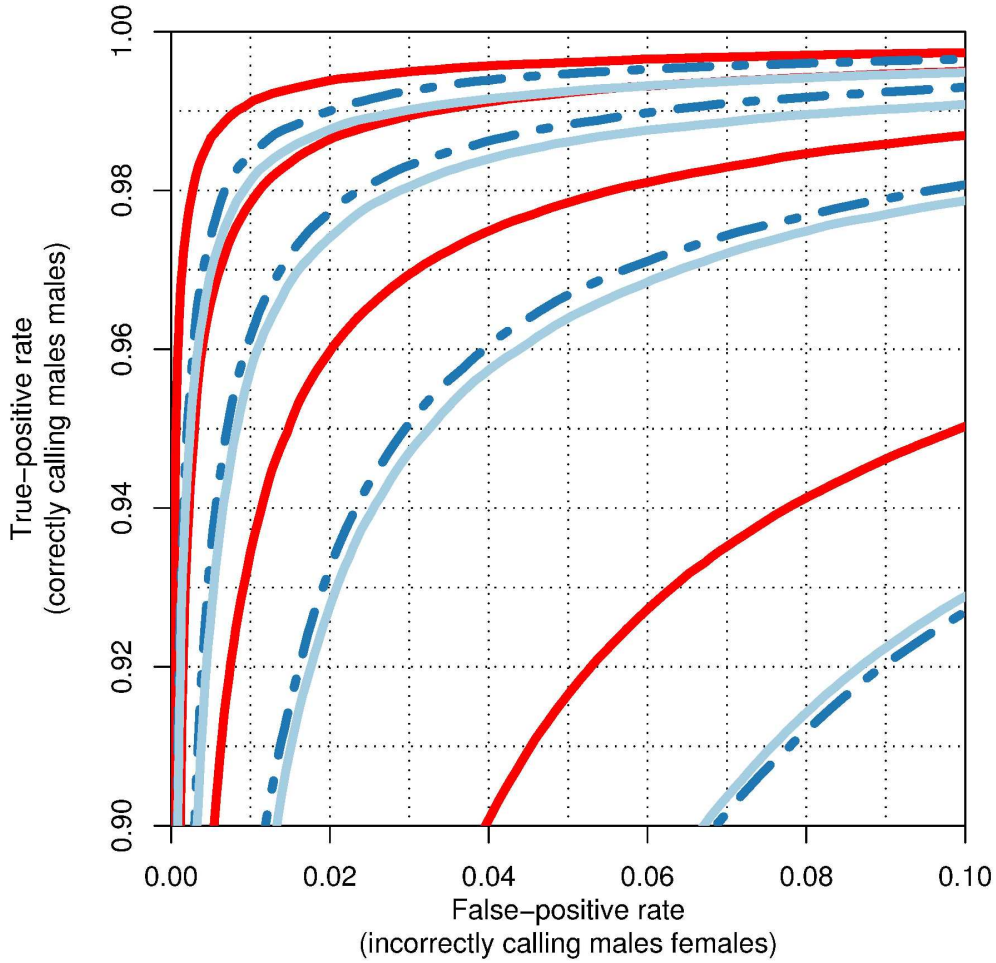

Performance on SNPs (left) and CN units (right) for CRMA v2 (solid red; left bars), CN5 (dashed blue; middle bars) and dChip* (solid light blue; right bars) when testing for CN=2 v. CN=1 (ChrX). The upper panels show the ROC curves for H=1,2,3,4 and the lower panels show the distribution of true-positive rates at fixed false-positive rate (1.72%).
152x152mm (600 x 600 DPI)

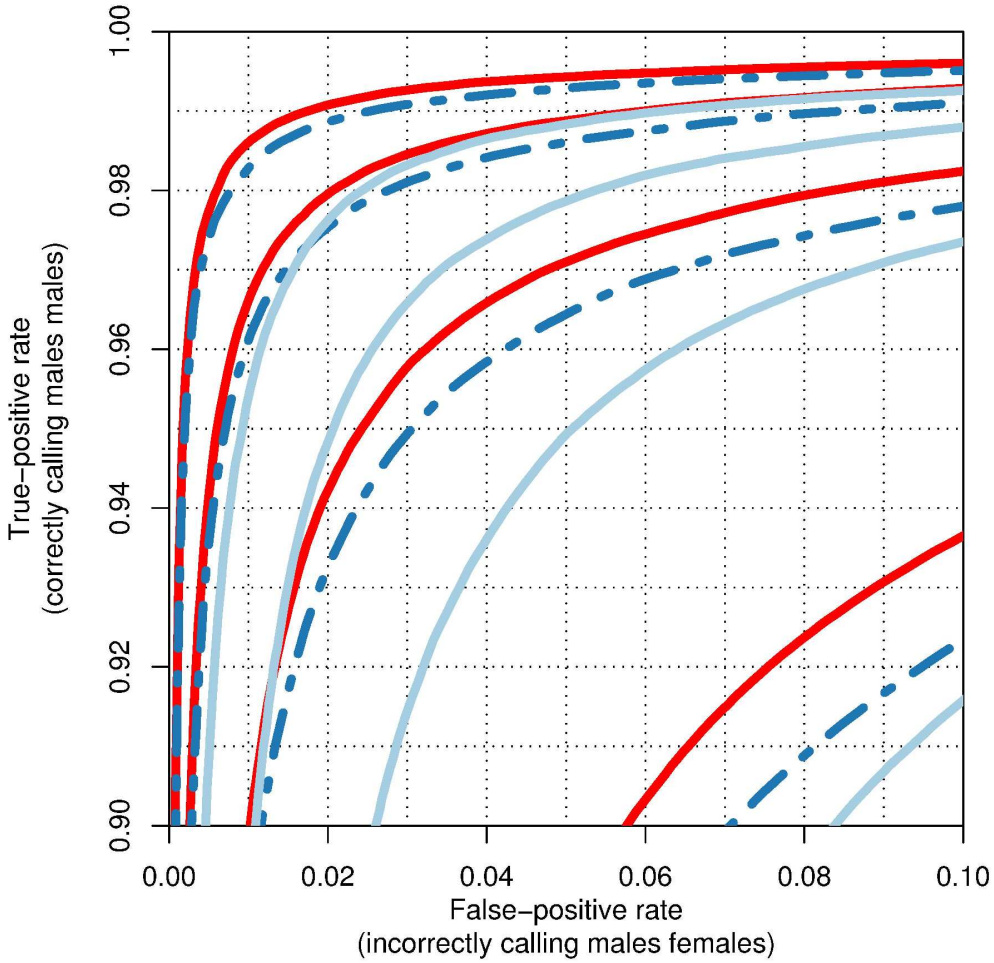

Performance on SNPs (left) and CN units (right) for CRMA v2 (solid red; left bars), CN5 (dashed blue; middle bars) and dChip* (solid light blue; right bars) when testing for CN=2 v. CN=1 (ChrX). The upper panels show the ROC curves for H=1,2,3,4 and the lower panels show the distribution of true-positive rates at fixed false-positive rate (1.72%).
152x152mm (600 x 600 DPI)

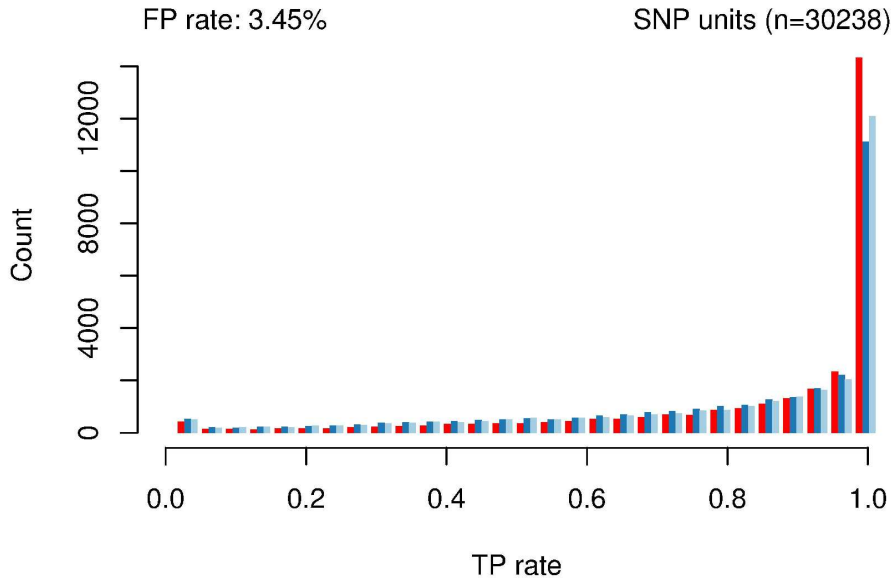

Performance on SNPs (left) and CN units (right) for CRMA v2 (solid red; left bars), CN5 (dashed blue; middle bars) and dChip* (solid light blue; right bars) when testing for CN=2 v. CN=1 (ChrX). The upper panels show the ROC curves for H=1,2,3,4 and the lower panels show the distribution of true-positive rates at fixed false-positive rate (1.72%).
152x94mm (600 x 600 DPI)

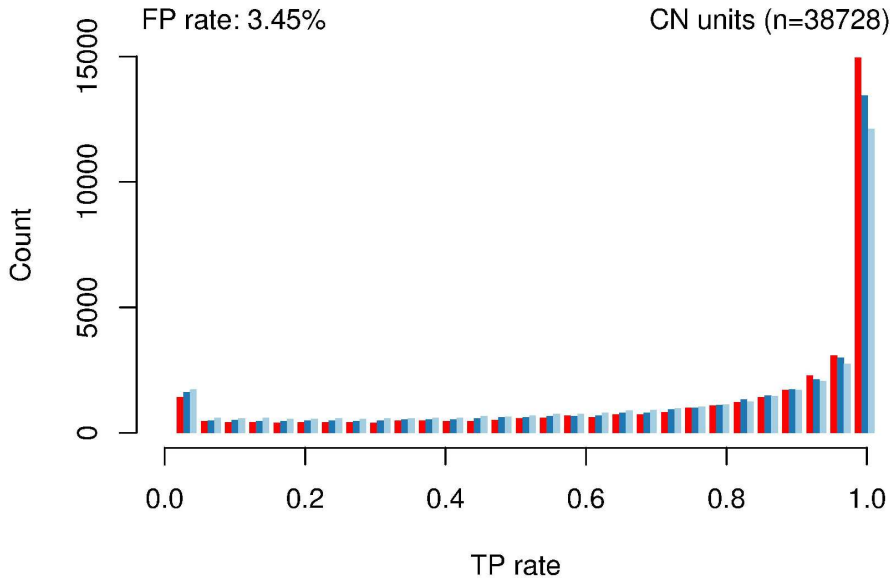

Performance on SNPs (left) and CN units (right) for CRMA v2 (solid red; left bars), CN5 (dashed blue; middle bars) and dChip* (solid light blue; right bars) when testing for CN=2 v. CN=1 (ChrX). The upper panels show the ROC curves for H=1,2,3,4 and the lower panels show the distribution of true-positive rates at fixed false-positive rate (1.72%).
152x94mm (600 x 600 DPI)

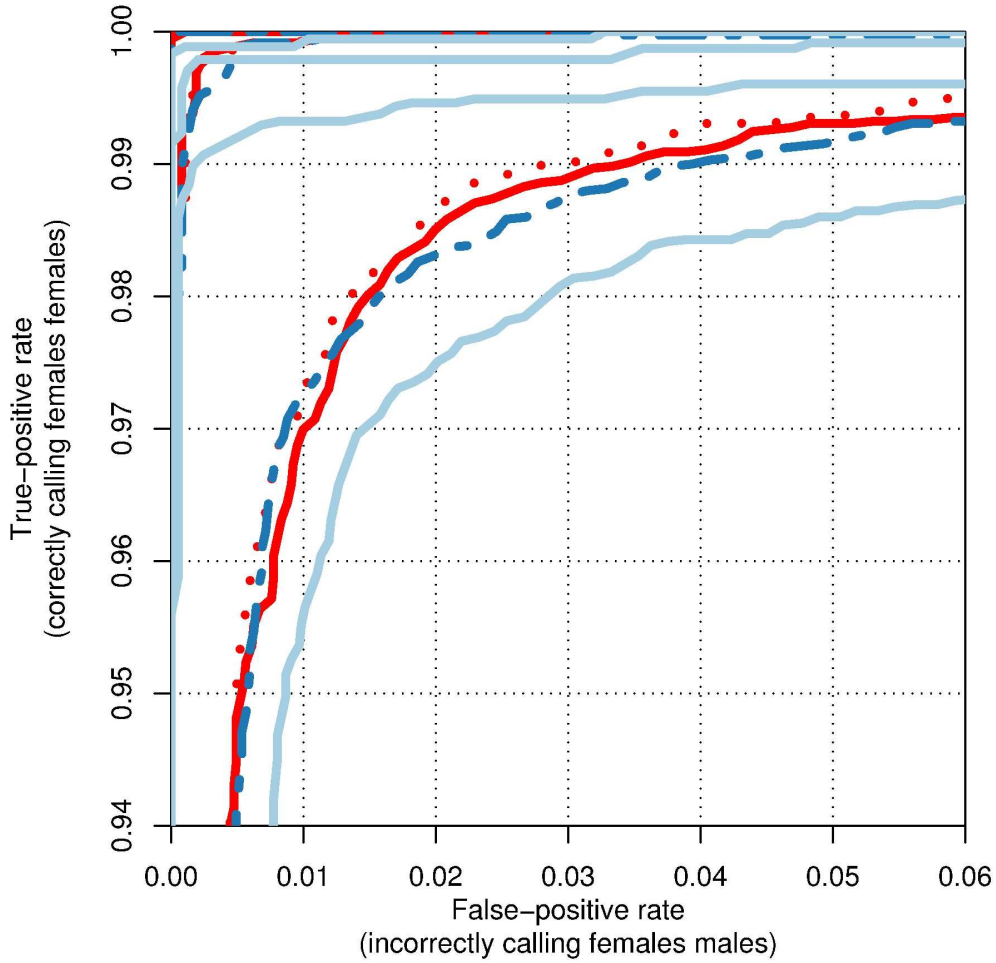

Performance on SNPs (left) and CN units (right) for CRMA v2, CN5 and dChip* when testing for CN=1 v. CN=0 (ChrY). The upper panels show the ROC curves for H=1,2,3,4 and the lower panels show the distribution of true-positive rates at fixed false-positive rate (1.72%). Legends as in Figure 4.
152x152mm (600 x 600 DPI)

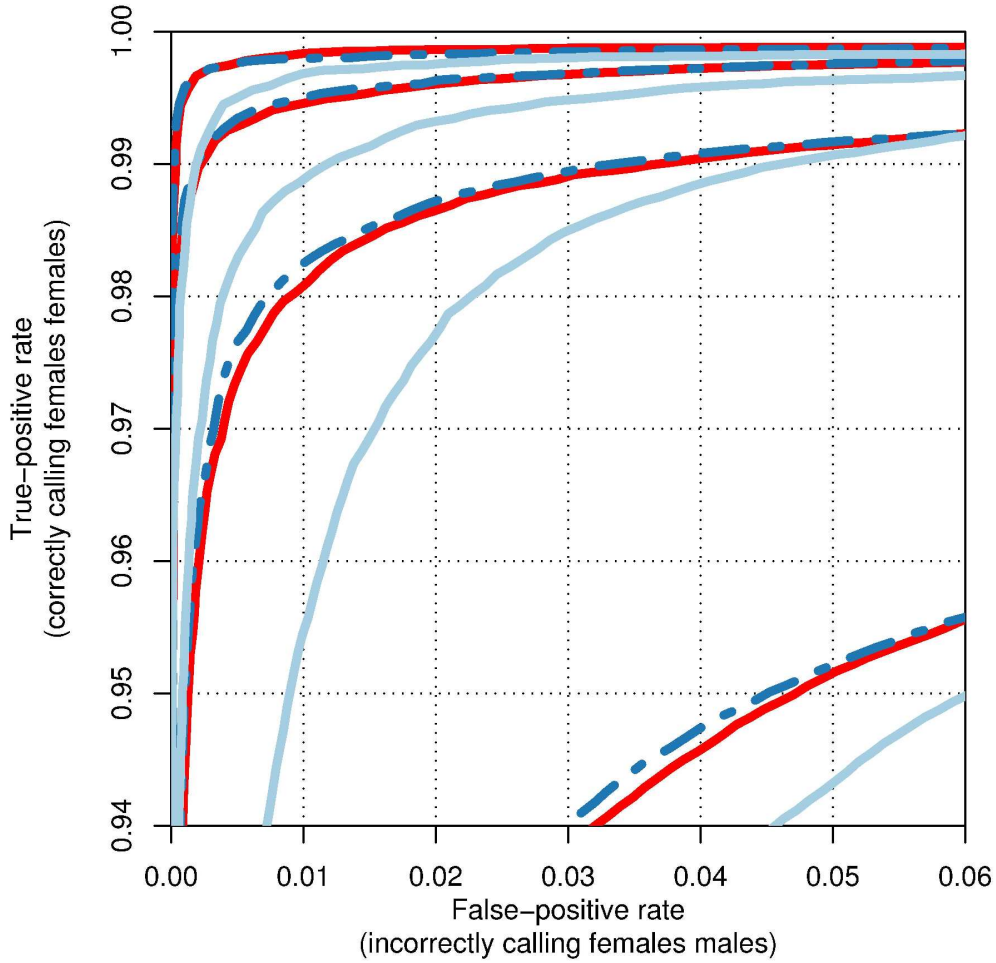

Performance on SNPs (left) and CN units (right) for CRMA v2, CN5 and dChip* when testing for CN=1 v. CN=0 (ChrY). The upper panels show the ROC curves for H=1,2,3,4 and the lower panels show the distribution of true-positive rates at fixed false-positive rate (1.72%). Legends as in Figure 4.
152x152mm (600 x 600 DPI)

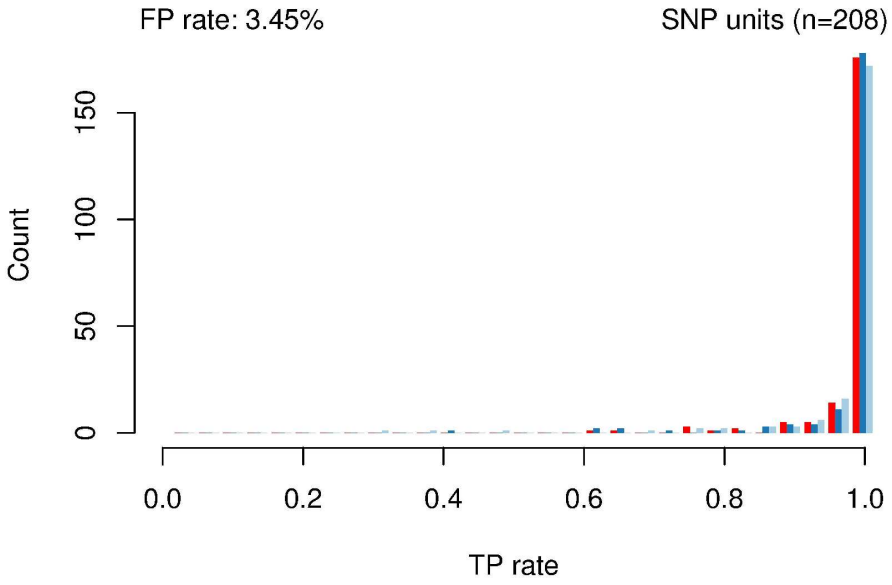

Performance on SNPs (left) and CN units (right) for CRMA v2, CN5 and dChip* when testing for CN=1 v. CN=0 (ChrY). The upper panels show the ROC curves for H=1,2,3,4 and the lower panels show the distribution of true-positive rates at fixed false-positive rate (1.72%). Legends as in Figure 4.
152x94mm (600 x 600 DPI)

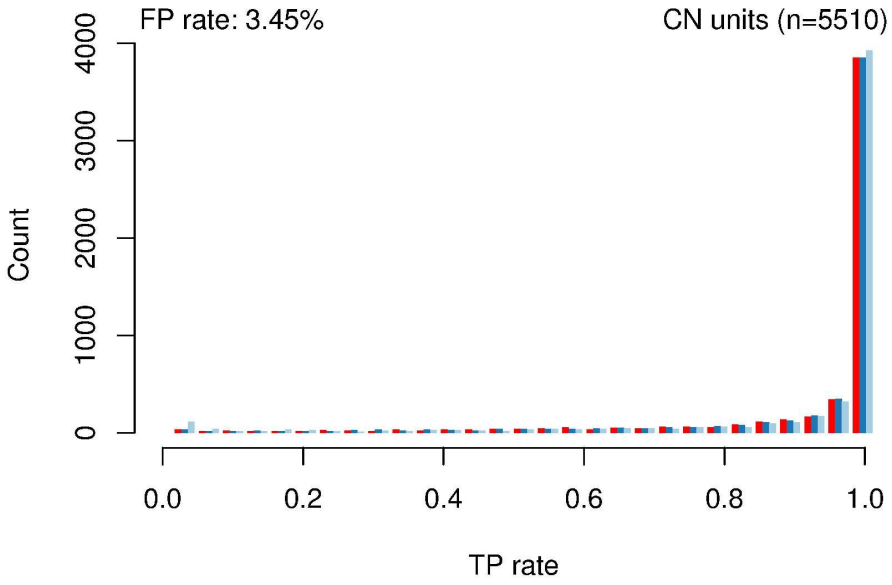

Performance on SNPs (left) and CN units (right) for CRMA v2, CN5 and dChip* when testing for CN=1 v. CN=0 (ChrY). The upper panels show the ROC curves for H=1,2,3,4 and the lower panels show the distribution of true-positive rates at fixed false-positive rate (1.72%). Legends as in Figure 4.
152x94mm (600 x 600 DPI)